Detailed description of the ENZ approach

Joseph J.M. Braat, Peter Dirksen, Augustus J.E.M. Janssen

E-mail addresses:

j.j.m.braat@tnw.tudelft.nl, peter.dirksen@philips.com, a.j.e.m.janssen@philips.com

1 The diffraction integral

An aberrated optical system is described by the pupil function $P(\rho, \theta)$. Because of the circular geometry that is present in most optical problems, we switch from the real-space cartesian coordinates (X, Y, Z) (see Fig. 1) to normalized cylindrical coordinates (ρ, θ, z) with $0 \leq \rho \leq 1$ and $0 \leq \theta \leq 2\pi$. A general pupil function can be written as

$$P(\rho, \theta) = A(\rho, \theta) \exp\{i\Phi(\rho, \theta)\} \ , \tag{1}$$

where A is the (non-negative) *transmission function* and Φ is the (real) *aberration phase*. Note that for our purpose we can consider the transmission function to be a possible nonuniformity in the beam that illuminates the entrance pupil of the optical system. In the case of a mirror system with a central obstruction, the transmission function A becomes zero in a central region.

From Fourier optics, see Ref.[1], Sec. 9.1, the normalized complex point-spread function $U(r, \phi; f)$ at a defocus plane described by focal parameter f and polar coordinates r, ϕ with $0 \leq r < \infty$ and $0 \leq \phi \leq 2\pi$, is given in normalized form as

$$U(r, \phi; f) = \frac{1}{\pi} \int_0^1 \int_0^{2\pi} \exp\{if\rho^2\} P(\rho, \theta) \exp\{2\pi i \rho r \cos(\theta - \phi)\} \, \rho d\rho d\theta \ . \tag{2}$$

Here the factor $\exp\{if\rho^2\}$ represents defocusing by the amount f and the $\exp\{2\pi\rho r \cos(\theta - \phi)\}$ is dictated by the Huygens-Fresnel principle under the usual approximations. The issue we consider here is how to compute U from P in a numerically reliable, accurate and convenient form. For this we shall in Sec. 2 consider the Zernike expansion of P and show in Sec. 3 how this expansion translates into an analytical expression for U.

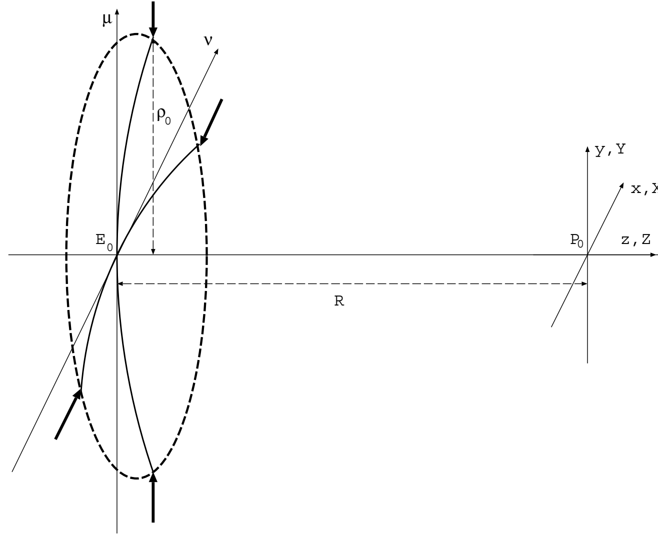

Figure 1: Geometry of the wave propagating from the exit pupil (center at E_0) towards the image plane (center at P_0). We use cylindrical coordinates instead of the cartesian set (X, Y, Z). The diameter of the exit pupil is $2\rho_0$ and the distance from pupil to image plane is R. In this document, the lateral coordinates on the exit pupil sphere are normalized to unity by means of the value of ρ_0 and denoted by (ν, μ); the corresponding normalized polar coordinates are (ρ, θ). The image plane coordinates (X, Y) are normalized with the aid of the diffraction unit, λ/s_0, and denoted by (x, y); $s_0 = \rho_0/R$ equals the image-side numerical aperture (NA) of the optical system. The corresponding polar coordinates in the image plane are (r, ϕ). The real-space axial coordinate Z is normalized with respect to the axial diffraction unit $u_0 = \frac{\lambda}{1-(1-s_0^2)^{1/2}}$. For optical systems with a low-to-moderate NA-value, $u_0 = 2\lambda/(NA)^2$.

2 Zernike representation of pupil functions

2.1 Classical viewpoint

Consider first the case that we have an optical system with only a pure-phase aberration, so that $P = \exp\{i\Phi\}$ with real Φ. Expand Φ into a *Zernike series*

$$\Phi(\rho, \theta) = \sum_{n,m} \alpha_n^m Z_n^m(\rho, \theta) \ , \tag{3}$$

with

$$Z_n^m(\rho, \theta) = R_n^m(\rho). \begin{cases} \cos m\theta \ , \\ \\ \sin m\theta \ . \end{cases} \tag{4}$$

Here the radial part $R_n^m(\rho)$ is the Zernike polynomial of *azimuthal* order m and *degree* n with integers $n, m \geq 0$ such that $n - m \geq 0$ and even, and α_n^m is the corresponding (real) expansion coefficient. We shall consider in the sequel only the cosine option

above, the sine option requiring just a second set of expansion coefficients.

The α_n^m carry physical significance, also see Ref.[1], Sec. 9.3, according to table 1 below.

Zernike terms				
$Z_0^0 = 1$	aberration-free (Z_1)		$Z_3^1 = (3\rho^3 - 2\rho)\cos\theta$	coma (Z_7)
$Z_1^1 = \rho\cos\theta$	tilt (Z_2)		$Z_2^2 = \rho^2\cos 2\theta$	astigmatism (Z_5)
$Z_2^0 = 2\rho^2 - 1$	defocus (Z_4)		$Z_4^0 = 6\rho^4 - 6\rho^2 + 1$	spherical (Z_9)

Table 1: Some characteristic lower-order Zernike terms; between parentheses the number of the Zernike polynomial is given according to the so-called fringe convention.

2.2 More general viewpoint

Consider a general pupil function $P = A\exp\{i\Phi\}$ and expand this product of functions into a Zernike series as

$$P(\rho,\theta) = A(\rho,\theta)\exp\{i\Phi(\rho,\theta)\} = \sum_{n,m}\beta_n^m Z_n^m(\rho,\theta)\ . \tag{5}$$

In the important special case that $A \approx 1$ and Φ is small, we have

$$P(\rho,\theta) \approx 1 + i\Phi(\rho,\theta) = 1 + \sum_{n,m} i\alpha_n^m Z_n^m(\rho,\theta)\ . \tag{6}$$

In the general case, the physical interpretation of the complex β_n^m may not be straightforward. There exists, however, a simple relationship between the on-axis intensity $I(0,0)$ of the diffraction image and the β-coefficients: $I(0,0) = |\beta_0^0|^2$. It is also possible to establish a slightly more elaborate expression for the frequently used Strehl intensity I_S in terms of the β-coefficients after normalization with respect to the integrated intensity over the pupil:

$$I_S = \frac{|\beta_0^0|^2}{\sum_{n,m}\left(\frac{|\beta_n^m|^2}{n+1}\right)}\ . \tag{7}$$

In the case that only weak phase aberrations are present, the $|\beta_n^m|$ $(n, m \neq 0)$ are close to zero and the Strehl intensity remains unity.

The strong point of the β-representation is that only a limited number of low order β's with modest amplitude is sufficient for the accurate description of the pupil function of a high-quality optical system. Going back from the β-representation to the α's with their easier physical interpretation in the wavefront domain implies a phase 'unwrapping' procedure. Phase unwrapping may lead to 2π ambiguities, especially if the phase function is not continuous. The majority of high-quality optical systems consists of well-corrected systems with relatively small β-values and the phase-unwrapping problem is easily solved.

3 From pupil function P to point-spread function U

3.1 Analytic solution

We insert the Zernike series representation of Sec. 2.2 for P into the diffraction integral and get for the point-spread function U the expression

$$U(r,\phi;f) = \sum_{n,m} \beta_n^m U_n^m(r,\phi;f) \quad , \tag{8}$$

where $\beta_n^m U_n^m$ is the contribution to U of the aberration term $\beta_n^m Z_n^m$. In [J1] it has been shown how to evaluate the U_n^m. There holds

$$U_n^m(r,\phi;f) = 2i^m V_n^m(r,f)\cos m\phi \, , \tag{9}$$

where

$$V_n^m(r,f) = \int_0^1 \exp\{if\rho^2\} R_n^m(\rho) J_m(2\pi r\rho)\rho d\rho \, , \tag{10}$$

with J_m the Bessel function of the first kind and of order m. For V_n^m there is the Lommel-type series expansion

$$V_n^m(r,f) = \exp(if) \sum_{l=0}^{\infty} \left(\frac{-if}{\pi r}\right)^l \sum_{j=0}^{p} u_{lj} \frac{J_{m+l+2j+1}(2\pi r)}{2\pi r} \tag{11}$$

in which $p = (n-m)/2$ and

$$u_{lj} = (-1)^p \, \frac{m+l+2j+1}{q+l+j+1} \binom{m+j+l}{l} \binom{j+l}{l} \binom{l}{p-j} \Big/ \binom{q+l+j}{l} \quad , \tag{12}$$

where $q = (n+m)/2$ and the binomial coefficients are defined for integer n, k by

$$\binom{n}{k} = \begin{cases} \frac{n!}{(n-k)!k!} & , \quad 0 \le k \le n \, , \\ 0 & , \quad \text{otherwise} \, . \end{cases} \tag{13}$$

3.2 Summary and features of analytic solution

Having expanded the complex pupil function P as

$$P(\rho,\theta) = \sum_{n,m} \beta_n^m R_n^m(\rho)\cos m\theta \, , \tag{14}$$

the defocused complex point-spread function U is given by

$$U(r,\phi;f) = 2\sum_{n,m} i^m \beta_n^m V_n^m(r,f)\cos m\phi \, . \tag{15}$$

Here the basic integrals V_n^m have the power-Bessel series representation

$$V_n^m(r,f) = \exp(if) \sum_{l=0}^{\infty} \left(\frac{-if}{\pi r}\right)^l \sum_{j=0}^{(n-m)/2} u_{lj} \frac{J_{m+l+2j+1}(2\pi r)}{2\pi r} \tag{16}$$

with explicitly given u_{lj}.

There are the following features of the solution.

i) Separation of the spatial and focal variables and the optical parameters r, ϕ, f, β_n^m.

ii) Numerical evaluation feasible for all r and all f with $|f|$ up to 25 (focal depth range approximately from -15 to 15).

iii) Easy and transparent computer codes; some downloadable examples of such codes, programmed in MatLab, are made available on the webpage under the heading *Downloads*.

iv) Lommel's solution (1886) for the aberration-free case and Nijboer's solution (1942) for the aberrated case at best focus $f = 0$ occur as special cases.

4 Aberration retrieval from the through-focus intensity point-spread function

In Sec. 3 we have seen how we can compute the through-focus complex amplitude U, and therefore the through-focus intensity $I = |U|^2$, from the Zernike expansion coefficients β of the pupil function P. We now consider the *inverse* problem, where we suppose the through-focus intensity I to be given and where we want to determine the pupil function P that gives rise to these intensity distributions. This is a problem of great practical importance since in the regime of optical frequencies occurring nowadays one generally has no access to the complex amplitude U while the intensity I is relatively easy to measure.

4.1 Approach

We postulate

$$P = P_{theory} = \sum_{n,m} \beta_n^m R_n^m(\rho) \cos m\theta \ , \tag{17}$$

and we estimate the unknown β_n^m by matching the given intensity $I(r, \phi; f)$ with the theoretical intensity

$$I_{theory}(r,\phi;f) = |U_{theory}(r,\phi;f)|^2 = \left| 2 \sum_{n,m} i^m \beta_n^m V_n^m(r,f) \cos m\phi \right|^2 \tag{18}$$

in the $(r, \phi; f)$-space (focal region). Since there is only a limited number of non-zero β's, this is a relatively easy task for which we give a work-out below under a "small" aberration assumption.

4.2 Work-out for small aberrations

We assume that aberrations are small. On the level of β's this means that β_0^0, the coefficient of the aberration-free term $Z_0^0 \equiv 1$, dominates the totality of all other β_n^m. Since we work with intensities, we may also assume that $\beta_0^0 > 0$, thereby fixing an undetermined overall phase factor. Then we get

$$
\begin{aligned}
|U_{theory}|^2 &= \left| 2\beta_0^0 V_0^0 + 2{\sum_{n,m}}' i^m \beta_n^m V_n^m \cos m\phi \right|^2 \\
&\approx 4(\beta_0^0)^2 |V_0^0|^2 + {\sum_{n,m}}' \beta_0^0 \mathrm{Re}(\beta_n^m).8\mathrm{Re}\left[i^m V_n^m V_0^{0*} \right] \cos m\phi \\
&\qquad - {\sum_{n,m}}' \beta_0^0 \mathrm{Im}(\beta_n^m).8\mathrm{Im}\left[i^m V_n^m V_0^{0*} \right] \cos m\phi \; .
\end{aligned} \tag{19}
$$

Here the $\approx$ refers to the fact that we have deleted small cross-terms (involving two β_n^m with $(n,m) \neq (0,0)$), and the $'$ on the summation signs means to indicate that the term with $(n,m) = (0,0)$ has been omitted. The β_n^m are found by optimizing the match between the above linearized theoretical intensity and the given or measured intensity in the focal region. Here we observe that the linearized theoretical intensity $|U_{theory}|^2$ involves the quantities $(\beta_0^0)^2$, $\beta_0^0\mathrm{Re}(\beta_n^m)$, $\beta_0^0\mathrm{Im}(\beta_n^m)$ in a linear way (with $\beta_0^0 > 0$), viz. as coefficients of the known and readily computable *basic functions*

$$
\begin{aligned}
RE_n^m(r,\phi;f) &= 8\mathrm{Re}\left[i^m V_n^m(r,f) V_0^{0*}(r,f) \right] \cos m\phi \; , \\
IM_n^m(r,\phi;f) &= 8\mathrm{Im}\left[i^m V_n^m(r,f) V_0^{0*}(r,f) \right] \cos m\phi \; .
\end{aligned} \tag{20}
$$

A convenient procedure results when the coefficients are chosen such that the mean squared difference between the given intensity and the linearized theoretical intensity is minimal. This works well in practice when a symmetric f-range is used and when sampling in the various image planes in the focal region is done in accordance with the polar nature of the coordinates r and ϕ. The β-representation has proven to be useful up to amplitude/phase values of typically 1.5 to 2 for an individual coefficient. The total effect of the β-coefficients on the Strehl intensity, see Eq.(7), should be such that there holds $I_S \geq 0.30$. Note that the Strehl intensity of a well-corrected optical imaging system should be at least 80%.

4.3 Features of the solution

There are the following particular features of the solution of the problem as outlined above:

i) Simple linear algebra with well-conditioned linear systems.

ii) Decoupling per azimuthal order ($\cos m\phi$!).

iii) Decoupling per real and imaginary part of β_n^m (RE_n^m and IM_n^m have opposite parity in f: symmetric f-range!).

iv) Additional "lucky breaks" in the often occurring case that we have a pure-phase aberration ($P = \exp\{i\Phi\} \approx 1 + i\Phi$). Then β_0^0=1 in the inversion scheme and all other β's are purely imaginary.

5 Advanced ENZ-theory

In the previous sections we have presented the basics of ENZ-theory for the computation of point-spread functions from pupil functions and the retrieval of aberrations from intensity point-spread functions in the focal region. When using ENZ-theory in practical situations, it may well happen that not all conditions under which the basic theory is supposed to be applied are met. We discuss in this section the extensions of the ENZ-theory that are required when we deal with

i) optical systems with high numerical aperture,

ii) (lithographic) systems with blurring in the image planes and focal stochastics,

iii) optical systems with aberrations exceeding the diffraction limit.

5.1 Optical systems with high numerical aperture (vector diffraction)

The original Extended Nijboer-Zernike diffraction analysis was limited to scalar optical fields, a good approximation for imaging systems with a numerical aperture smaller than 0.60. At larger numerical aperture, several complications are encountered that have been partly treated in the literature:

i) the vector character of the light has to be accounted for because the focal field can not be described by a single quantity. In general, if the light is linearly polarized in the x-direction at the entrance of the optical system, we will also observe a dominating x-component in the focal region. But on top of this, non-negligible field components in the y- and z-direction will be measured. The calculation of each of these components requires a special diffraction integral that is more complicated than the original scalar version.

ii) the distribution of the intensity on the exit pupil of the optical system sphere is, apart from a lateral magnification factor, not a simple one-to-one mapping of the intensity distribution on the entrance pupil. One has to specify the type of optical system to determine the exact mapping. In the frequently occurring case of imaging systems with a large image field (the so-called aplanatic optical systems), a special mapping is found that leads, with respect to the lateral pupil coordinate, to an increasing intensity towards the rim of the exit pupil. This radiometric effect is of minor importance at low aperture but needs to be incorporated in the high numerical aperture case.

iii) the defocusing of a high NA pencil of light is not simply described by multiplying the various integrands of the diffraction integrals with a quadratic phase

factor. The phase departure of a defocused beam is proportional to the perpendicular pathlength difference between two spherical caps. Apart from the leading quadratic term, higher order terms need to be incorporated in the expression for the defocus effect.

iv) the vectorial diffraction integrals that were given in the literature did not allow an analytic treatment with respect to separate Zernike aberration terms. It has turned out to be possible to develop semi-analytic expressions for the basic vectorial diffraction integrals for each Zernike aberration term like it was demonstrated earlier for the scalar diffraction case. With the foregoing extensions to the scalar case we have obtained analytic expressions for the electric and magnetic field components in the focal region of a high-NA imaging system ([J4]).

The next step was to create a backward calculation scheme for the vectorial case so that the aberrations and transmission defects of a high NA optical system can be retrieved. Although the scheme, including the retrieval of the so-called 'polarisation aberration', comprises rather lengthy expressions, the retrieval at high numerical aperture has become feasible (see [J7]) and is currently applied both to synthetic data for testing purposes and to experimental data; in the latter case, only a special illumination with natural light was available and this leads to a rather drastically reduced version of our retrieval scheme.

We now list some of the changes and extensions that occurred in the formulae when switching from the scalar case to the high-NA case, including the introduction of the vector diffraction formalism. In the case of optical systems with a numerical aperture exceeding 0.60, the focal factor $\exp[if\rho^2]$ in the diffraction integral (2) fails to be an accurate approximation of the true focal factor $A_R(\rho)exp[i\Phi_c(\rho)]$ in which

$$A_R(\rho) = (1 - NA^2\rho^2)^{-\frac{1}{4}} \;\; , \;\; \Phi_c(\rho) = f\frac{1-(1-NA^2\rho^2)^{\frac{1}{2}}}{1-(1-NA^2)^{\frac{1}{2}}} \;\; . \tag{21}$$

In (21), A_R is an amplitude function accounting for the radiometric effect and Φ_c is the phase function that correctly describes defocusing in the exit pupil. In [J6], Sec. 5, it is shown how the ENZ-theory can be simply extended to give adequate forward computation and retrieval results in the regime $0.60 \leq NA \leq 0.80$. For values of NA in excess of 0.80, this extension is not adequate anymore; moreover one has to adopt a vectorial treatment of the imaging and also the state of polarization of the used light should be taken into account. We consider, for the case of $NA \geq 0.80$, the complex pupil function on the exit pupil, according to

$$B^x = A^x \exp[2\pi i W^x] \;\; , \;\; B^y = A^y \exp[2\pi i W^y] \;\; , \tag{22}$$

with A^x and A^y the field strenghts in the x and y directions and W^x and W^y the wavefront aberrations in units of λ, the wavelenght of the polarized light. These B^x and B^y are expanded in series involving the Zernike terms $\exp[im\theta]R_n^{|m|}(\rho)$ with coefficients $\beta_{n,x}^m$ and $\beta_{n,y}^m$, where we adopt now for notational convenience the exponential rather

than the trigonometric notation for the θ-dependence. The vector corresponding to the field arising from an initially linearly x-polarized incident wave is given by

$$\mathbf{E}^x(r,\phi,f) = -i\gamma s_0^2 \exp\left[\frac{-if}{u_0}\right] \sum_{n,m} i^m \beta_{n,x}^m \exp\left[im\phi\right] \times \left(\begin{array}{c} V_{n,0}^m + \frac{s_0^2}{2} V_{n,2}^m \exp\left[2i\phi\right] + \frac{s_0^2}{2} V_{n,-2}^m \exp\left[-2i\phi\right] \\ -\frac{is_0^2}{2} V_{n,2}^m \exp\left[2i\phi\right] + \frac{is_0^2}{2} V_{n,-2}^m \exp\left[-2i\phi\right] \\ -is_0 V_{n,1}^m \exp\left[i\phi\right] + is_0 V_{n,-1}^m \exp\left[-i\phi\right] \end{array} \right) . \quad (23)$$

Here we have written

$$s_0 = NA = \sin\alpha \ , \ u_0 = 1 - \sqrt{1-s_0^2} \ , \ f = -2\pi u_0 \frac{z}{\lambda} \ , \quad (24)$$

with α the aperture angle of the system and z the axial coordinate in units of λ. A similar expression results for the case of an initially y-polarized incident wave. For full details, see [J4], [J7]. The $V_{n,j}^m$ functions occurring in (23) are given as

$$V_{n,j}^m = \int_0^1 \frac{\rho^{|j|}\left(1+\sqrt{1-s_0^2\rho^2}\right)^{-|j|+1}}{(1-s_0^2\rho^2)^{1/4}} \exp\left[\frac{if}{u_0}\left(1-\sqrt{1-s_0^2\rho^2}\right)\right] \times R_n^{|m|}(\rho) J_{m+j}(2\pi r\rho)\rho d\rho \ . \quad (25)$$

The computation of the $V_{n,j}^m$ has been described in [J4], Appendix B, see also Subsec. 5.4 below; in [J4], Sec. 5, a number of figures, showing moduli of field components computed according to (23-25) under a variety of polarization conditions are presented. In [J7], the above forward computation scheme is taken as a point of departure to devise a retrieval method for both aberrations and birefringence for which a detailed and instrumental graphical illustration of the arising basic functions is presented. In [C4], [P10] the results of forward calculation using the vectorial high-NA formulas and those using the low-NA formulas are compared for the case of unpolarized light. Moreover, for this unpolarized case, aberration retrieval under high-NA conditions is performed.

5.2 Image blur and focal stochastics

In the lithographic application of aberration retrieval according to the ENZ-method, the recorded intensities $I'(r,\phi;f)$ are quite often a smeared version of the actual intensities $I(r,\phi;f)$. Common reasons for this smearing are

i) mechanical noise in the horizontal planes,

ii) acid diffusion in the image planes during the post exposure baking process (resist-based recording),

iii) stochastic variation of the focal parameter f.

It is customary to model the combined effects of the position noise and the diffusion in the image planes with the aid of a Gaussian convolution kernel with zero mean and radial symmetry. Furthermore, the focal parameter is assumed to have Gaussian distribution around its nominal value. Accordingly, the relation between the recorded intensity I' and the actual intensity I is

$$I'(x,y;f) = \iiint I(x,y;f)d(x-x',y-y')f_n(f-f')dx'dy'df' \quad . \tag{26}$$

Here d and f_n are given by

$$d(x,y) = \frac{1}{2\pi\sigma_r^2}\exp\left(-\frac{x^2+y^2}{2\sigma_r^2}\right) \quad , \qquad real\ x,y \quad , \tag{27}$$

and

$$f_n(f) = \frac{1}{\sigma_f\sqrt{2\pi}}\exp\left(\frac{-f^2}{2\sigma_f^2}\right) \qquad , \qquad real\ f \quad , \tag{28}$$

with σ_r and σ_f the standard deviations in the spatial domain and focal range respectively. In the retrieval scheme, it is necessary to correct the basic functions RE_n^m and IM_n^m of (20) in accordance with the integral operation in (26), where we assume the blurring effect to be linear. The numerical evaluation of the integrals in (26), with $I = RE_n^m$ or IM_n^m, is a time-consuming and delicate matter, especially when σ_r and σ_f are small. In [J8] this problem is circumvented by identifying σ_r and σ_f with diffusion times t and s according to

$$\sigma_r = \sqrt{2Dt} \quad , \quad \sigma_f = \sqrt{2cs} \quad , \tag{29}$$

with D and c diffusion constants. The recorded intensity $I'(x,y;f)$ can then be considered as the result $I(x,y;f;t,s)$ of the diffusion proces after times t, s with initial intensity $I(x,y;f;0,0)$ equal to the actual intensity $I(x,y;f)$. This diffused function $I = I(x,y;f;t,s)$ satisfies the diffusion equations

$$\frac{\partial I}{\partial t} = D\left(\frac{\partial^2}{\partial x^2}+\frac{\partial^2}{\partial y^2}\right)I \quad , \quad \frac{\partial I}{\partial s} = c\frac{\partial^2 I}{\partial f^2} \quad . \tag{30}$$

The $I(x,y;f;t,s)$ can then be approximated as

$$\begin{aligned} I(x,y;f;t,s) &= I(x,y;f;0,0) + t\frac{\partial I}{\partial t}(x,y;f;0,0) + s\frac{\partial I}{\partial s}(x,y;f;0,0) \\ &+ \frac{1}{2}t^2\frac{\partial^2 I}{\partial t^2}(x,y;f;0,0) + ts\frac{\partial^2 I}{\partial t\partial s}(x,y;f;0,0) + \frac{1}{2}s^2\frac{\partial^2 I}{\partial s^2}(x,y;f;0,0) \\ &+ \ \ldots \end{aligned} \tag{31}$$

in which the required partial derivatives can de evaluated in accordance with (30). In [J8], the resulting approximations have been calculated analytically for $I = RE_{n=2p}^{m=0}$,

$IM_{n=2p}^{m=0}$. We have, for instance, for $|V_0^0|^2$ the first order corrected expression (with σ_r and σ_f reinstalled according to (29))

$$\begin{aligned} |V_0^0|^2 \quad &- \quad \pi^2\sigma_r^2\left(2|V_0^0|^2 + 2\mathrm{Re}\left(V_2^0V_0^{0*}\right) - 4|V_1^1|^2\right) \\ &- \quad \frac{1}{2}\sigma_f^2\left(\frac{1}{6}|V_0^0|^2 + \frac{1}{3}\mathrm{Re}\left(V_4^0V_0^{0*}\right) - \frac{1}{2}|V_2^0|^2\right) \quad . \end{aligned} \tag{32}$$

In Sec. 5.4 below we shall sketch a more systematic approach for evaluating Laplacians and $\frac{\partial}{\partial f}$ of basic functions.

5.3 Retrieval of larger aberrations: predictor-corrector approach

In (19) we have linearized $|U_{theory}|^2$ with respect to terms involving products $\beta_0^0\mathrm{Re}(\beta_n^m)$, $\beta_0^0\mathrm{Im}(\beta_n^m)$. This is a valid approach when the totality of all β_n^m with $(n,m) \neq (0,0)$ is relatively small compared to β_0^0. For larger aberrations it is better to adopt a predictor-corrector approach. Here a sequence $\beta_n^m(k)$, $\quad k = 0, 1, \ \ldots$, of estimates for the β_n^m is constructed in which $\beta_n^m(0)$ is the result of the matching procedure described in Subsec. 4.2. The estimate $\beta_n^m(k+1)$ is obtained from $\beta_n^m(k)$ by applying the matching procedure with the recorded intensity corrected for the kth estimate

$$4 \sum_{n_1,m_1;n_2,m_2}{}^{\prime\prime} \quad \mathrm{Re}\left[\beta_{n_1}^{m_1}(k)\beta_{n_2}^{m_2*}(k)i^{m_1-m_2}V_{n_1}^{m_1}V_{n_2}^{m_2*}\right]\cos m_1\varphi \cos m_2\varphi \tag{33}$$

of the small-cross-terms contribution where the $''$ at the summation sign refers to the totality of all n_1, m_1, n_2, m_2 with $(n_1, m_1) \neq (0,0) \neq (n_2, m_2)$. In [J6] this procedure has been worked out in simulation, and it was found that aberrations well exceeding the diffraction limit could be perfectly retrieved.

5.4 The general integral

The general basic function, as occurs in (33), in its high NA-version, as we have it in (25), involves the product of an integral

$$\begin{aligned} J(k,j,l;E) = \qquad & i^l \int_0^1 \rho^k \left(1 + \sqrt{1 - s_0^2\rho^2}\right)^{-j+1} \quad \times \\ & E(\rho)\exp\left[\frac{if}{u_0}\left(1 - \sqrt{1 - s_0^2\rho^2}\right)\right] J_l(2\pi\rho r)\rho d\rho e^{il\phi} \end{aligned} \tag{34}$$

with the complex conjugate of another such integral. Here $E(\rho)$ is a relatively smooth function of ρ, such as

$$\frac{1}{(1 - s_0^2\rho^2)^{\frac{1}{4}}} \frac{J_1(b\rho)}{\frac{1}{2}b\rho} R_n^m(\rho). \tag{35}$$

The factor $\left(1 - s_0^2\rho^2\right)^{-\frac{1}{4}}$ represents the radiometric effect. The factor $J_1(b\rho)/\frac{1}{2}b\rho$ represents a second amplitude non-uniformity that occurs when the pinhole used for producing the point-spread functions has a non-negligible diameter b (normalized). The factor $R_n^m(\rho)$ is a Zernike polynomial of moderate degree n.

The integrals J transform conveniently under applying the Laplacian $\Delta = \frac{\partial^2}{\partial x^2} + \frac{\partial^2}{\partial y^2}$ or partial derivatives ∂_x, ∂_y, ∂_f. There holds

$$\begin{aligned}
\Delta J(k,j,l;E) &= -4\pi^2 J(k+2,j,l;E) \ , && (36)\\
\partial_x J(k,j,l;E) &= \pi i J(k+1,j,l+1;E) + \pi i J(k+1,j,l-1;E) \ , && (37)\\
\partial_y J(k,j,l;E) &= \pi J(k+1,j,l+1;E) - \pi J(k+1,j,l-1;E) \ , && (38)\\
\partial_f J(k,j,l;E) &= \frac{is_0^2}{u_0} J(k+2,j+1,l;E) \ . && (39)
\end{aligned}$$

Hence, in the case of high-NA imaging with image blur and focal stochastics, the terms that occur in (31) via (30), are all expressible in terms of the general integral J. In [J4], Appendix B, a method has been given to evaluate integrals J, but this method is still rather complicated. We are presently devising a more user-friendly computation scheme that should be used when the degree n of the Zernike polynomial R_n^m involved in E is not too large.

6 Survey of literature and applications ENZ

The ENZ-theory started with [J1] in which the power-Bessel series of the Lommel type for the diffraction integral involving a general aberration term Z_n^m is presented. This paper [J1] was followed immediately by [J2] where the solution of the forward problem was treated (calculation of the through-focus point-spread function from the pupil function using its Zernike expansion). In [J2] the merits of the new approach for forward calculations are established from an optical point of view and a rule-of-thumb is developed for the number of terms one should include in the infinite power-Bessel series (normally $3|f|$ suffices). The extension of the forward calculation to more complicated object structures is considered and the influence of the illumination coherence is included for a simple two-point resolution test.

In [J5] a different series expansion for the basic general diffraction integral is presented. These alternative expansions involve products of two types of Bessel functions and arise when Bauer's formula expressing $\exp\{if\rho^2\}$ as an infinite series involving products of spherical Bessel functions $j_k(f/2)$ and Zernike polynomials $R_{2k}^0(\rho)$ of order $m=0$, is used in conjunction with relatively new results from the theory of orthogonal polynomials. In particular, the important problem, see Ref.[1], pp. 534-535, of systematically writing the product of two Zernike polynomials of order m_1, m_2 as a linear combination of Zernike polynomials of order m_1+m_2 can be solved with these recent results. The resulting Bessel-Bessel series representation generalizes a result of the "classical" Nijboer-Zernike theory for the aberration-free case $m=n=0$. Bessel-Bessel series representations are somewhat more complicated than the representations of the Lommel type, but have the advantage that they are practically immune to loss of digits, irrespective how large f and/or r are.

In [J4] the Zernike-based solution for the forward problem is extended to cover the case of aberrated, high-aperture optical systems. In this extension, the focal factor $\exp\{if\rho^2\}$ is replaced by its correct version $\exp\{(if/u_0)[1-(1-s_0^2\rho^2)^{1/2}]\}$ with

$u_0 = 1 - (1 - s_0^2)^{1/2}$ and $s_0 = NA$, the numerical aperture of the system. Furthermore, the radiometric effect, manifesting itself by a factor $(1 - s_0^2\rho^2)^{-1/4}$ by which the pupil function must be multiplied, is accounted for. Moreover, in [J4], the vector character of the electromagnetic field is taken into account, including the state of polarization of the light used. In [J4], the squared modulus of the field is displayed as well as the spatial distribution of the Poynting vector in the focal region. These results were also presented in part at two scientific meeting, see [P2], [P4].

The papers [J1], [J2] on the solution of the forward problem were soon followed by a contribution at the SPIE Microlithography 2002 conference [C1] on the solution of the inverse problem of aberration retrieval; an extended version of [C1] is the journal paper [J3]. In [C1] and [J3] the proof-of-principle of the aberration retrieval method is given for the case of small pure-phase aberrations in a practical lithographic setting. Also, there is briefly hinted at the method for retrieval of general aberrations. The various "lucky breaks" that occur for the pure-phase version, such as immunity to deletion of small cross-terms in the theoretical intensity and only third-order errors due to linearizing $\exp\{i\Phi\}$ as $1 + i\Phi$, were noted in [C1], [J3]. Furthermore, the forward and backward solutions are corrected for the realistic situation that the pinhole that is being imaged has a finite size (instead of being a true delta function). This is simply done by replacing the (real) focus value f in $\exp\{if\rho^2\}$ by a complex value $f + id$, where d is directly related to the diameter of the pinhole. A basic survey of the ENZ-approach, both for the forward problem and the inverse problem, with some emphasis on applications in a lithographic context, is presented in [C5].

Further validations of the aberration retrieval method are given in [C2] where experimental results, achieved on a modern wafer scanner, are shown. In particular, [C2] contains pictures that show retrieval results for aberrated lithographic lenses to which specific pure-phase aberrations of known size were intentionally added.

A further extension of the retrieval methodology in lithography is the inclusion of the effects of spatial diffusion and of focal statistics. This requires appropriate modification of the basic functions RE_n^m, IM_n^m in the retrieval equations. Some details for this are given in [C3], where diffusion parameters and focal variances are estimated along with spherical aberration coefficients. An extended and considerably more detailed version of [C3] is [J8]. In the latter manuscript, the correction of the basic functions corresponding to radially symmetric aberrations is done analytically to second order for the leading basic function involving $|V_0^0|^2$ and to first order for the basic functions involving the $V_{2p}^0 V_0^{0*}$ with $p = 1, 2, ..$, see (20). This avoids the numerical evaluation of the required convolution integrals which is a time-consuming and delicate matter, especially when the diffusion parameters and focal variances are small. In addition, in [C6] we discuss the application of ENZ to aerial image based lens metrology and lens adjustment, the experimental results pertaining to a prototype DUV lens ($NA = 0.75$, $\lambda = 248$ nm). In this application, the ENZ-method has been adjusted for chromatic errors in accordance with the corrections discussed above. There is good agreement with results obtained from an interferometric experiment, where the ENZ-method has the advantage that both phase AND transmission errors are estimated.

The aberration retrieval methods have also been validated by performing exten-

sive simulations in [J6]. Here the "lucky breaks" that occur for the pure-phase retrieval method are explained and illustrated by consideration of special aberrations $1+i\alpha_n^m Z_n^m$, $\exp\{i\alpha_n^m Z_n^m\}$. These "lucky breaks" do not occur, however, for the case of generally aberrated pupil functions. For the latter case, an iterative version of the method is proposed in which in each iteration step the deleted small cross-terms are estimated and included in the procedure by feeding back the β's from the previous step. It is observed in [J6] that then perfect reconstruction occurs for aberrations that may well exceed the diffraction limit. Furthermore, a simple but effective procedure is developed in [J6] to account in the diffraction integral for effects like the use of pinholes of finite size and the radiometric effect.

An extension of the general aberration retrieval method has been presented in [J7] where the high-NA effects have been included in accordance with the vector diffraction theory. Although the formulae that describe the through-focus intensity have a quite complicated nature, it is again possible to extract the harmonic azimuthal functions in the theoretical expression for the intensity in the focal region. Not only the geometrical aberration and transmission errors of the optical system but also the birefringence effects are of importance now. By collecting the data from four through-focus intensity maps, it is, in principle, possible to retrieve the complete 'polarization' aberrations of a high-NA optical system. Like in the scalar diffraction case, it is possible to establish an equation for the vector diffraction case in which the measured through-focus intensity distribution is approximated by a linearized analytic expression for the intensity containing the unknown Zernike coefficients (see [T1] and [J9]). The incident light can have arbitrary polarization; successive intensity measurements with orthogonal linear and/or circular polarization states allow the retrieval of the polarization aberrations of the system. An iterative scheme has also been applied in the vector diffraction case and it was demonstrated that Zernike coefficients converge to a final stable value once they are bound to an interval of typically one wavelength or 2π in the phase domain. As a special case, we discuss in [C4] (and [J8]) the extension of aberration retrieval to high-NA optical systems if the pin-hole source is illuminated with unpolaried light and the aberrations are restricted to be circularly symmetric. A simplified version of the vector diffraction analysis can be used here and it has been applied to experimental data pertaining to an immersion scanner (NA=0.85, λ=193 nm).

Various presentations on the aberration retrieval methods were given at scientific meetings, see [P3], [P5], [P6], [P7], [P8], [P9,abstract], [P9,poster], [P10], [P11], [P12], [P13], [P14], [T1].

7 Future extensions

Several long-term options for further research on the ENZ-theory are envisaged at this moment.

i) **High-NA aberration retrieval**

The retrieval operations so far have been limited to the scalar diffraction case; the method now has to be extended to the case of high-NA optical systems. The

forward problem for the high-NA case is already considerably more complicated than the low-NA forward problem, and this is reflected in the inverse problem by a corresponding increase in complexity, see [J7]. At this moment, the first results of high-NA retrieval have been obtained with 'synthetic data'. With this expression we mean that analytically obtained intensity data in the focal volume (ENZ forward calculation) have been used to replace the measured data that eventually are needed to go back to the aberrations and transmission defects of an optical system. The next step is to use measured intensity data that have been obtained for a variety of incident states of polarization. In this way we can go back not only to geometrical aberrations of the optical system but also to its birefringence properties ('polarization aberrations'). However, for the case that the used light may be assumed to be unpolarized (which up to now is a realistic assumption in the lithographic practice) and the aberrations may be assumed to be radially symmetric, a simplification occurs so that the resulting retrieval scheme strongly resembles the scheme that was found for the low-NA systems. These developments are to be found in [J7], [C4]. A further enhancement of the general retrieval method consists of incorporating and using the iterative option of the general method. This option has been applied to the high-NA case with synthetic data and leads to exact solutions after a modest number of iterations (typically 5 to 10). The application of the iterative procedure to an experimental set-up as encountered in lithographic applications is the logical next step.

ii) **Fast and accurate forward calculation (extended object)**

A new field of application can be found in the forward calculation of more complicated object structures as encountered in optical lithography. The optimum resist image with an as large as possible tolerance against image plane off-set (critical dimension or 'CD'-control in lithography) has to be calculated. To this goal, on top of the basic geometrical features, fine structure is introduced and iteratively adjusted on the object mask (or reticle). Instead of using the small point-source that was the starting point in the ENZ-theory, we now switch to extended objects that are not necessarily illuminated in a coherent way. More in particular, the partial coherence of the illumination of the object mask is a parameter to be optimized for obtaining the best resist image. The iterative process of image optimization is carried out using Hopkins' partial coherence theory of image formation that is based on Fourier methods and their numerical implementation. With the high-NA effects included, this method becomes very slow. An analytic tool like the ENZ-theory can be of great value because of its basic inherent accuracy, quick convergence and analytic decomposition of the focal intensity distribution along the three axis of the cylindrical coordinate system.

iii) **Imaging in electron microscopy**

Further possible applications could be found in high-resolution electron microscopy operating close to the diffraction limit. Both aberration retrieval and the measurement of the far-field intensity distribution of sources could be of interest.

iv) **Aperture synthesis imaging**

The coherent behaviour of arrays of apertures could also be characterized by a Zernike expansion of the transmission function of the synthetic aperture and its composite aberration pattern, constructed from the individual apertures and their mutual wavefront piston and tilt errors. The application will necessarily be limited to relatively 'dense' aperture geometries. Very 'dilute' synthetic apertures will pose serious convergence problems with respect to the Zernike expansion.

v) **Stochastic imaging (atmospheric perturbations)**

Imaging through turbulent media (e.g. astronomical observation through the atmosphere) has been analyzed using Zernike expansions of the stochastic wavefront function. Correction of the atmospheric turbulence using adaptive optics requires the derivation of an optical error signal that allows the mirror deformation of the adaptive optical element to counteract the atmospheric perturbation. ENZ-theory is capable of accurately analyzing the (heavily) aberrated through-focus point source images that are produced by the atmospheric perturbation. The retrieval method then produces the steering signal for the deformable optical element.

8 Computer codes

Some basic computer codes (MatLab-based) have been made available on the ENZ-webpage.

References

[1] M. Born and E. Wolf, *Principles of Optics* (4th rev. ed., Pergamon Press, New York, 1970).

9 ENZ-publications

Journal papers

J1.
A.J.E.M. Janssen, "Extended Nijboer-Zernike approach for the computation of optical point-spread functions," J. Opt. Soc. Am. A 19 (2002), pp. 849-857.
J2.
J.J.M. Braat, P. Dirksen, A.J.E.M. Janssen, "Assessment of an extended Nijboer-Zernike approach for the computation of optical point-spread functions," J. Opt. Soc. Am. A 19 (2002), pp. 858-870.

J3.
P. Dirksen, J.J.M. Braat, A.J.E.M. Janssen, C.A.H. Juffermans, ”Aberration retrieval using the extended Nijboer-Zernike approach,” Journal of Microlithography, Microfabrication, and Microsystems 2 (2003), pp. 61-68.
J4.
J.J.M. Braat, P. Dirksen, A.J.E.M. Janssen, A. van de Nes, ”Extended Nijboer-Zernike representation of the field in the focal region of an aberrated high-aperture optical system,” J. Opt. Soc. Am. A 20 (2003), pp. 2281-2292; also in Virtual Journal of Biological Physics Research 6 (2003), issue 12.
J5.
A.J.E.M. Janssen, J.J.M. Braat, P. Dirksen, ”On the computation of the Nijboer-Zernike aberration integrals at arbitrary defocus,” J. Mod. Opt. 51 (2004), pp. 687-703.
J6.
C. van der Avoort, J.J.M. Braat, P. Dirksen, A.J.E.M. Janssen, ”Aberration retrieval from the intensity point-spread function in the focal region using the extended Nijboer-Zernike approach,” J. Mod. Opt. 52 (2005), pp. 1695-1728.
J7.
J.J.M. Braat, P. Dirksen, A.J.E.M. Janssen, S. van Haver, A.S. van de Nes, ”Extended Nijboer-Zernike approach to aberration and birefringence retrieval in a high-numerical-aperture optical system,” J. Opt. Soc. Am. A 22 (2005), pp. 2635-2650.
J8.
P. Dirksen, J.J.M. Braat, A.J.E.M. Janssen, ”Estimating resist parameters using the Extended Nijboer-Zernike theory,” Journal of Microlithography, Microfabrication, and Microsystems 5 (2006), 013005, pp. 1-11.
J9.
S. van Haver, J.J.M. Braat, P. Dirksen, A.J.E.M. Janssen, ”High-NA aberration retrieval with the Extended Nijboer-Zernike vector diffraction theory,” J. Eur. Opt. Soc. -RP 1 (2006), 06004, pp. 1-8.
J10.
A.J.E.M. Janssen, P. Dirksen, ”Concise formula for the Zernike coefficients of scaled pupils,” Journal of Microlithography, Microfabrication, and Microsystems 5 (2006), 030501, pp. 1-3.

Conference Proceedings

C1.
P. Dirksen, J.J.M. Braat, P. De Bisschop, A.J.E.M. Janssen, C.A.H. Juffermans, Alvina Williams, ”Characterization of a projection lens using the extended Nijboer-Zernike approach,” Proc. SPIE 4691, Santa Clara, March 2002, pp. 1392-1399.
C2.
P. Dirksen, J. Braat, A.J.E.M. Janssen, C. Juffermans, A. Leeuwestein, ”Experimental determination of lens aberrations from the intensity point-spread function in the focal region,” Proc. SPIE 5040, Santa Clara, February 2003, pp. 1-10.

C3.
P. Dirksen, J. Braat, A.J.E.M. Janssen, A. Leeuwestein, H. Kwinten, D. Van Steenwinckel, "Determination of resist parameters using the extended Nijboer-Zernike theory," Proc. SPIE 5377, Santa Clara, February 2004, pp. 150-159.
C4.
P. Dirksen, J.J.M. Braat, A.J.E.M. Janssen, A. Leeuwestein, "Aberration retrieval for high-NA optical systems using the extended Nijboer-Zernike theory," Proc. SPIE 5754, San Jose, USA, February-March 2005, pp. 262-273.
C5.
J.J.M. Braat, P. Dirksen, A.J.E.M. Janssen, "Through-focus point-spread function evaluation for lens metrology using the extended Nijboer-Zernike theory," in Fringe 2005 (W. Osten, ed.), Springer, Berlin, 2005, pp. 299-307.
C6.
P. Dirksen, J.J.M. Braat, A.J.E.M. Janssen, A. Leeuwestein, T. Matsuyama, T. Noda, "Aerial image based lens metrology for wafer steppers," Proc. SPIE 6154, San Jose, February 2006, 61540X, pp. 1-11.

Presentations at scientific meetings

P1.
P. Dirksen, J.J.M. Braat, P. De Bisschop, A.J.E.M. Janssen, C.A.H. Juffermans, A. Leeuwestein, "Characterization of a projection lens using the extended Nijboer-Zernike approach", SPIE conference on Microlithography, Santa Clara, March 3-8, 2002.
P2.
J.J.M. Braat, P. Dirksen, A.J.E.M. Janssen, A. van de Nes, "Extended Nijboer-Zernike representation of the field in the focal region of an aberrated high-aperture optical system, poster presented at the Annual Meeting of OSA, Orlando, October 2002.
P3.
P. Dirksen, J.J.M. Braat, A.J.E.M. Janssen, C. Juffermans, A. Leeuwestein, "Experimental determination of lens aberrations from the intensity point-spread function in the focal region," SPIE conference on Microlithography, February 23-28, 2003.
P4.
J.J.M. Braat, P. Dirksen, A.J.E.M. Janssen, A.S. van de Nes, "Extended Nijboer-Zernike description of the high-aperture focal field created by a beam with angular momentum", presented at Focus on Microscopy 2003, Genova, April 13-16, 2003.
P5.
P. Dirksen, J.J.M. Braat, A.J.E.M. Janssen, A. Leeuwestein, H. Kwinten, D. van Steenwinckel, "Determination of resist parameters using the extended Nijboer-Zernike theory," SPIE conference on Microlithography, February 21-26, 2004.
P6.
J.J.M. Braat, P. Dirksen, A.J.E.M. Janssen, A.S. van de Nes, "Quality assessment of focusing optics by aberration retrieval using the extended Nijboer-Zernike diffraction theory", presented at Focus on Microscopy 2004, Philadelphia, April 4-7, 2004.

P7.
P. Dirksen, J.J.M. Braat, A.J.E.M. Janssen, D. van Steenwinckel, A. Leeuwestein, "Aberration retrieval for a lithographic lens in the presence of focus variation and spatial diffusion," IISB Lithography Simulation Workshop, Hersbruck, Germany, September 17-19, 2004.
P8.
J.J.M. Braat, P. Dirksen, A.J.E.M. Janssen, "Extended Nijboer-Zernike analysis for vectorial diffraction calculations and aberration retrieval," IISB Lithography Simulation Workshop, Hersbruck, Germany, September 17-19, 2004.
P9.
J.J.M. Braat, P. Dirksen, A.J.E.M. Janssen, A.S. van de Nes, "Complex pupil function reconstruction using the extended Nijboer-Zernike diffraction theory," abstract presented at OSA Annual Meeting, October 2004, Rochester, USA; corresponding poster presentation: "Complex pupil function reconstruction at high numerical aperture using the extended Nijboer-Zernike diffraction theory".
P10.
P. Dirksen, J.J.M. Braat, A.J.E.M. Janssen, A. Leeuwestein, "Aberration retrieval for high-NA optical systems using the Extended Nijboer-Zernike theory," SPIE conference on Microlithography, San Jose, February 27 - March 4, 2005.
P11.
J.J.M. Braat, P. Dirksen, A.J.E.M. Janssen, A. van de Nes, "Polarisation-aberration retrieval for high-NA systems using the extended Nijboer-Zernike diffraction theory", presented at Focus on Microscopy 2005, Jena, March 20-24, 2005.
P12.
J.J.M. Braat, P. Dirksen, A.J.E.M. Janssen, "Through-focus point-spread function evaluation for lens metrology using the Extended Nijboer-Zernike theory", presented at Fringe 2005, Stuttgart, September 12-14, 2005.
P13.
J.J.M. Braat, P. Dirksen, A.J.E.M. Janssen, A. Leeuwestein, T. Matsuyama, T. Noda, "Aerial image based lens metrology for wafer steppers," SPIE conference on Microlithography, San Jose, February 19-24, 2006.
P14.
S. van Haver, J.J.M. Braat, P. Dirksen, A.J.E.M. Janssen, "High-NA lens characterization by through-focus intensity measurements," to be presented at EOS Annual Meeting 2006, Paris, October 16-19, 2006.

Master's thesis

T1.
S. van Haver, "Extended Nijboer-Zernike diffraction and aberration retrieval theory for high-numerical-aperture optical imaging systems," January 2005.

All references in this text can be found at the Extended Nijboer-Zernike website itself: Extended Nijboer-Zernike (ENZ) Analysis and Aberration Retrieval.